

## Renormalization Group Approach To Error-Correcting Codes

Jonathan S. Yedidia\* and Jean-Philippe Bouchaud†

TR-2001-19    October 2018

### Abstract

We explain an algorithm that approximately but efficiently assesses particular parity-check error-correcting codes of large, but finite, blocklength. This algorithm is based on the “renormalization-group” approach from physics: the idea is to continually replace an error-correcting code with a simpler error-correcting code that has nearly identical performance, until the code is reduced to a small enough size that its performance can be computed exactly. This assessment algorithm can be used as a subroutine in a more general algorithm to search for optimal error-correcting codes of specified blocklength and rate.

This work may not be copied or reproduced in whole or in part for any commercial purpose. Permission to copy in whole or in part without payment of fee is granted for nonprofit educational and research purposes provided that all such whole or partial copies include the following: a notice that such copying is by permission of Mitsubishi Electric Information Technology Center America; an acknowledgment of the authors and individual contributions to the work; and all applicable portions of the copyright notice. Copying, reproduction, or republishing for any other purpose shall require a license with payment of fee to Mitsubishi Electric Information Technology Center America. All rights reserved.

Copyright © Mitsubishi Electric Information Technology Center America, 2018  
201 Broadway, Cambridge, Massachusetts 02139

---

\* MERL, 201 Broadway, Cambridge MA 02139. [yedidia@merl.com](mailto:yedidia@merl.com)

† SPEC CEA-Saclay, Orme des Merisiers, 91191 Gif Sur Yvette, France. [bouchaud@spec.saclay.cea.fr](mailto:bouchaud@spec.saclay.cea.fr)

1. May 2001 Draft version
2. June 2001 Current version

# 1 Introduction

A fundamental problem in the field of information theory is the design of optimal or nearly optimal error-correcting codes of given block-length and rate that can also be decoded practically. This problem can now be considered essentially solved in the small blocklength (e.g.  $N < 100$ ) and very large blocklength (e.g.  $N > 10^6$ ) regimes. However, error-correcting codes that are used in practical situations (for example, for wireless communication) typically have blocklengths in an intermediate regime (around  $N = 2000$ ). (The reason that intermediate blocklength codes are used in practice is that larger blocklength codes have better performance, but have a longer decoding time, so one will normally choose the code with the largest blocklength for which the 'lag' caused by decoding is still tolerable.)

In the small blocklength regime, classical coding theory, as summarized in textbooks such as [1], provides a panoply of codes of different blocklengths and rates, many of which are known to be optimal or nearly optimal. As long as the blocklength is small enough, these codes can be also be decoded practically (and optimally) using maximum-likelihood decoders.

In the last few years, the problem of finding good codes in the very large blocklength regime has been essentially solved but in a very different way; by focusing on parity-check codes defined using sparse (generalized) parity check matrices [2]. These kinds of codes were first introduced by Gallager in 1962 [3], but were not properly appreciated until recently. In the last eight years, however, new and improved codes defined by sparse generalized parity check matrices (such as turbocodes [4, 5], irregular low-density parity check (LDPC) codes [6, 7, 8, 9, 10], Kanter-Saad codes [11, 12, 2], repeat-accumulate codes [13], and irregular repeat-accumulate codes [14]) have been the object of intense study. Such codes have three particularly noteworthy advantages. First, they can be efficiently decoded using belief propagation (BP) iterative decoding [15]. Secondly, their performance can often be theoretically analyzed in the infinite-blocklength limit using the *density evolution* approach [16]. Finally, using the density evolution approach, or through simulations, one can demonstrate that these codes are good codes, in the sense that in the infinite-blocklength limit, BP decoding will perfectly decode all message blocks that have a noise level below some threshold level, and that threshold level is often not too far from the Shannon limit.

In recent years, a favored way to design new codes has thus been to

optimize codes for the infinite blocklength limit using density evolution, and to hope that a scaled-down version would still be a good code [7, 9, 10, 14]. The problem with this approach is that for  $N < 10^4$  at least, we are still noticeably far from the infinite-blocklength limit. In particular, simulations will find many decoding failures at noise levels far below the threshold level predicted by infinite blocklength calculations. Furthermore, there will not necessarily even exist a way to scale down the codes derived from the density evolution approach. For example, the best known irregular LDPC codes at a given rate (in the  $N \rightarrow \infty$  limit) will often have variable nodes that should participate in hundreds or even thousands of parity checks [10], which obviously makes no sense if the overall number of parity checks is 100 or less. When one wants to make real codes of finite blocklength, one is therefore often forced to choose a code which is sub-optimal in the infinite-blocklength limit, with no theoretical guidance.

Our goal, which is achieved by the renormalization group approach described here, has therefore been to develop an assessment algorithm more powerful than the ordinary density evolution approach, which will predict, at least approximately, the decoding failure rate as a function of the noise level for a specific code of finite blocklength. It is important to realize that for finite blocklengths, one does not expect perfect decoding below any particular threshold noise level, so that to evaluate a code, one now needs a whole performance curve rather than a single number (the critical noise threshold) as might be computed in the density evolution approach.

The outline of the rest of this paper is as follows. In the next section, we review the density evolution approach for the binary erasure channel, where it is particularly simple. We pay particular attention to codes defined on trees, for which the density evolution approach becomes exact. Section 3 is the heart of the paper, where we introduce and explain our renormalization-group (RG) approach. We show how it recovers exact answers for codes defined on trees, and give a procedure, which can be made increasingly accurate at the cost of more computational power to handle codes defined on graphs with loops. We present some numerical results comparing our RG calculations with simulations of realistic finite blocklength codes in section 4. In section 5, we explain how to extend the RG approach to the Additive White Gaussian Noise (AWGN) channel. In section 6, we speculate on how one might use our RG algorithm as a sub-routine for a more general algorithm for the design of codes.

## 2 The density evolution approach for the binary erasure channel (BEC)

The density evolution approach is analytically very simple for the binary erasure channel. [6, 17] Since this approach is important background for our own RG approach, we will review it in this section.

### 2.1 Parity check codes

We will begin by studying linear block binary codes which can be defined in terms of an ordinary parity check matrix. In a parity check matrix  $A$ , the columns represent transmitted variable bits, while the rows define linear constraints between the variable bits. More specifically, the matrix  $A$  defines a set of valid vectors (codewords)  $z$ , such that each component of  $z$  is 0 or 1, and

$$Az = 0 \tag{1}$$

where we assume all multiplication and addition is modulo 2.

If a parity check matrix has  $N$  columns and  $N - k$  rows it will represent a code of blocklength  $N$  and rate  $k/N$  (unless some of the rows are not linearly independent, in which case some of the parity checks are redundant, and the code will actually be of higher rate).

For each parity check matrix, there is a corresponding Tanner graph representation. [18] A Tanner graph is a bipartite graph with two kinds of nodes: variable nodes (which we denote by circles) and check nodes (denoted by squares). In a Tanner graph, each check node is connected to the variable nodes that represent the bits involved in that check. For example, the parity check matrix

$$A = \begin{pmatrix} 1 & 1 & 0 & 1 & 0 & 0 \\ 1 & 0 & 1 & 0 & 1 & 0 \\ 0 & 1 & 1 & 0 & 0 & 1 \end{pmatrix} \tag{2}$$

corresponds to the Tanner graph shown in figure 1.

Codes represented by parity check matrices are “linear,” which means that all the codewords are linear combinations of other codewords. There will be  $2^k$  codewords, each of length  $N$ ; e.g., for the example given above, the codewords are 000000, 001011, 010110, 011101, 100110, 101101, 110011, 111000. Because of the linearity property, we may use any of the codewords

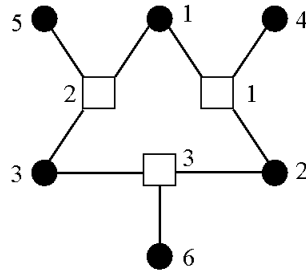


Figure 1: Tanner graph for a simple error-correcting code.

as a representative; throughout this paper, we will always assume that the all-zeros codeword is transmitted.

## 2.2 Belief propagation decoding in the BEC

The binary erasure channel is a binary input channel with three output symbols: a 0, a 1, and an erasure, which can be represented by a question mark  $?$ . The input symbol will pass through the channel as an erasure with probability  $x$  and will be received correctly with probability  $1 - x$ . It is important to note that the BEC never flips bits from 0 to 1 or vice versa. If we assume that the all-zeros codeword is transmitted, all received words will thus consist entirely of zeros and erasures.

We will assume that the receiver decodes using a belief propagation (BP) decoder with discrete messages. A message  $m_{ia}$  will be sent from each variable node  $i$  to each check  $a$  that it participates in, with the message representing information about the state of the variable node. In general, the message can be in one of three states: 1, 0, or  $?$ , but since we assume that the all-zeros state is always transmitted, we can ignore the possibility that  $m_{ia}$  has value

1.

Similarly, there will be a message  $m_{ai}$  sent from each check node  $a$  to all the variable nodes  $i$  that participate in that check. These messages should be interpreted as directives from the check to the variable node about what state it should be in, based on the states of the other variable nodes participating in the check. The check-to-bit messages can again in principle take on the values 0, 1, or ?, but again only the two messages 0 and ? will be relevant when the all-zeros codeword is transmitted.

In the BP decoding algorithm for the BEC, a message  $m_{ia}$  from a variable node to a check node will be equal to a non-erasure received message (because such messages are always correct in the BEC), or to an erasure if all incoming messages are erasures. A message  $m_{ai}$  from a check node  $a$  to a variable node  $i$  will be an erasure if any incoming message from another node participating in the check is an erasure, otherwise it will take on the value of the binary sum of all incoming messages from other nodes participating in the check.

The BP decoding algorithm is an iterative algorithm. One should initialize the messages so that all variable nodes that are not erased send out messages equal to the corresponding received bit, and all other messages are initially erasures. Iterating the BP message equations, one will eventually always converge to stationary messages (convergence of BP decoding algorithms is guaranteed for the particularly simple BEC, but not for other channels). The final decoded value of any erased variable node is just the value of any non-erasure message coming into that node, unless there is no incoming non-erasure message, in which case the BP decoding algorithm gives up and fails to decode that particular variable node.

### 2.3 Density evolution

We now consider the average of BP decoding over many blocks. Associated with each message  $m_{ia}$ , we introduce a real number  $p_{ia}$  which represents the probability that the message  $m_{ia}$  is an erasure. Similarly, we associate with each message  $m_{ai}$  a real number  $q_{ai}$  which represents the probability that the message  $m_{ai}$  is an erasure.

In the density evolution approach, we compute the probabilities  $p_{ia}$  and  $q_{ai}$  in a way that is exact as long as the Tanner graph representing the code

has no loops. We take

$$p_{ia} = x \prod_{b \in N(i) \setminus a} q_{bi} \quad (3)$$

where  $b \in N(i) \setminus a$  represents all check nodes that neighbor variable node  $i$  except for check node  $a$ . This equation can be derived from the fact that for a message  $m_{ia}$  to be an erasure, the variable node  $i$  must be erased in transmission, and all incoming messages from other checks must be erasures as well. Of course, if the incoming messages were correlated, this equation would not be correct, but on a Tanner graph with no loops, each incoming message is independent of the others.

Similarly, we find that

$$q_{ai} = 1 - \prod_{j \in N(a) \setminus i} (1 - p_{ja}) \quad (4)$$

which can be derived (again assuming incoming messages are uncorrelated) from the fact that a message  $q_{ai}$  will only be in a 0 or 1 state if all incoming messages are in a 0 or 1 state.

The density evolution equations (3) and (4) can be solved by iteration. A good initialization is  $p_{ia} = x$  for all messages from variable nodes to check nodes and  $q_{ai} = 0$  for all messages from check nodes to variable nodes, as long as one begins the iteration with the  $q_{ai}$  messages. The BEC density evolution equations should ultimately converge (this can be guaranteed for codes defined on graphs without loops). One can finally compute  $b_i$ , which is the probability of a failure to decode at variable node  $i$ , from the formula

$$b_i = x \prod_{a \in N(i)} q_{ai} \quad (5)$$

## 2.4 Exact solution of a small code

As mentioned, the density evolution equations (3), (4), and (5) should be exact when the code has a Tanner graph representation without loops. Let us work through a small example, to see how this works. We consider the code with parity check matrix

$$A = \begin{pmatrix} 1 & 1 & 0 & 0 \\ 0 & 1 & 1 & 1 \end{pmatrix} \quad (6)$$

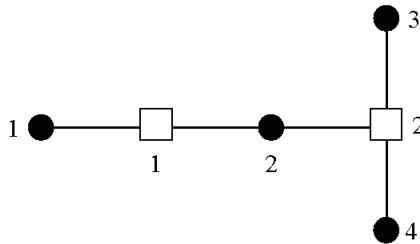


Figure 2:

and a corresponding Tanner graph shown in figure 2.

This code has four codewords: 0000, 0011, 1101, and 1110. If the 0000 message is transmitted, there will be sixteen possible received messages: 0000, 000?, 00?0, 00??, 0?00, and so on. The probability of receiving a particular message with  $n_e$  erasures is  $x^{n_e}(1-x)^{(4-n_e)}$ . Messages might be partially or completely decoded by a BP decoder; for example the received message ?00? will be fully decoded to 0000, but the message 0???? will only be partially decoded to 00??, because there is not enough information to determine whether the transmitted codeword was actually 0000 or 0011.

We can easily compute the exact probability that a given bit will remain an erasure after decoding by summing over the sixteen possible received messages weighted by their probabilities. For example, the first bit will only be decoded as an erasure if one of the following messages are received: ???0, ??0?, or ???? , so the total probability that the first bit will not be decoded is  $2x^3(1-x) + x^4 = 2x^3 - x^4$ . If we focus on the last bit instead, we find that it will be decoded unless one of the following messages is sent: 00??, 0????, ?0??, ??0? or ???? , so the overall probability that the fourth bit is not decoded will be  $x^2(1-x)^2 + 3x^3(1-x) + x^4 = x^2 + x^3 - x^4$ .

In the density evolution approach, we need to solve equations for the following variables:  $p_{11}$ ,  $p_{21}$ ,  $p_{22}$ ,  $p_{32}$ ,  $p_{42}$ ,  $q_{11}$ ,  $q_{12}$ ,  $q_{22}$ ,  $q_{23}$ ,  $q_{24}$ ,  $b_1$ ,  $b_2$ ,  $b_3$ , and  $b_4$ . The equations are:

$$p_{11} = x \quad (7)$$

$$p_{21} = xq_{22} \quad (8)$$

$$p_{22} = xq_{12} \quad (9)$$

$$p_{32} = x \quad (10)$$

$$p_{42} = x \quad (11)$$

$$q_{11} = p_{21} \quad (12)$$

$$q_{12} = p_{11} \quad (13)$$

$$q_{22} = 1 - (1 - p_{32})(1 - p_{42}) \quad (14)$$

$$q_{23} = 1 - (1 - p_{22})(1 - p_{42}) \quad (15)$$

$$q_{24} = 1 - (1 - p_{22})(1 - p_{32}) \quad (16)$$

and

$$b_1 = xq_{11} \quad (17)$$

$$b_2 = xq_{12}q_{22} \quad (18)$$

$$b_3 = xq_{23} \quad (19)$$

$$b_4 = xq_{24} \quad (20)$$

Solving these equations, we find

$$p_{11} = x \quad (21)$$

$$p_{21} = 2x^2 - x^3 \quad (22)$$

$$p_{22} = x^2 \quad (23)$$

$$p_{32} = x \quad (24)$$

$$p_{42} = x \quad (25)$$

$$q_{11} = 2x^2 - x^3 \quad (26)$$

$$q_{12} = x \quad (27)$$

$$q_{22} = 2x - x^2 \quad (28)$$

$$q_{23} = x + x^2 - x^3 \quad (29)$$

$$q_{24} = x + x^2 - x^3 \quad (30)$$

and

$$b_1 = 2x^3 - x^4 \quad (31)$$

$$b_2 = 2x^3 - x^4 \quad (32)$$

$$b_3 = x^2 + x^3 - x^4 \quad (33)$$

$$b_4 = x^2 + x^3 - x^4. \quad (34)$$

Examining the results for  $b_1$  and  $b_4$ , we see that the density evolution solution agrees exactly with the direct approach for this code.

## 2.5 The large blocklength limit

If we assume that all local neighborhoods look identical, we can simplify the density evolution equations. For example, if each variable node belongs to  $d_v$  parity checks, and each check node is attached to  $d_c$  variable nodes, then we can take all the  $p_{ia}$  equal to the same value  $p$ , all the  $q_{ai}$  equal to the same value  $q$ , and all  $b_i$  equal to the same value  $b$ . We then find

$$p = xq^{d_v-1} \quad (35)$$

$$q = 1 - (1 - p)^{d_c-1} \quad (36)$$

and

$$b = xq^{d_v} \quad (37)$$

which are the density evolution equations for  $(d_v, d_c)$  *regular Gallager codes*, valid in the  $N \rightarrow \infty$  limit. A regular Gallager code [3] is a code defined by a sparse random parity check matrix characterized by the restriction that each row has exactly  $d_c$  1's in it, and each column contains exactly  $d_v$  1's. The intuitive reason that these equations are valid in the infinite blocklength limit is that as  $N \rightarrow \infty$ , the size of typical loops in the Tanner graph of a regular Gallager code will also go to infinity, so all incoming messages to a node will be independent, and a regular Gallager code will behave like a code defined on a graph without loops.

If we solve equations (35) and (36) for specific values of  $d_v$  and  $d_c$ , we find that below a critical erasure threshold  $x_c$ , the solution is  $p = q = b = 0$ , which means that decoding is perfect. Above  $x_c$ ,  $b$  will have a non-zero solution, which correspond to decoding failures.  $x_c$  is easy to determine numerically. For example, if  $d_v = 3$  and  $d_c = 5$ , then  $x_c \approx 0.51757$ .

These density evolution calculations can be generalized to irregular Gallager codes [6], or other codes like irregular repeat-accumulate codes [14] which have a finite number of different classes of nodes with different neighborhoods. In this generalization, one derives a system of equations, typically with one equation for the messages leaving each class of node. By solving the system of equations, one can again find a critical threshold  $x_c$ , below which decoding is perfect. Such codes can thus be optimized in the  $N \rightarrow \infty$  limit by finding the code that has maximal noise threshold  $x_c$ . Simulations of such codes with very large blocklengths agree quite well with the density evolution predictions.

Unfortunately, the density evolution approach is useless, or at least misleading, for codes with finite blocklength. One might think that one could solve equations (3) and (4) for any finite code, and hope that ignoring the presence of loops one is not too important a mistake. This does not work out, as one can simply see by considering regular Gallager codes. Equations (3), (4), and (5) for a finite blocklength regular Gallager code will have exactly the same solutions as one would find in the infinite-blocklength limit, so one would not predict *any* finite-size effects. Simulations, on the other hand, show that the real performance of finite-blocklength regular Gallager codes is considerably different (and worse) than that predicted by such a naive approach.

## 3 The renormalization group approach

### 3.1 Intuition

The basic idea behind the “real-space” renormalization group approach from physics [19] is very similar to the idea behind recursion from computer science. To evaluate the performance of a large but finite code, we try to replace the code with a slightly smaller code with the same performance. In particular, at each step in the process, we keep a Tanner graph and a set of  $p_{ia}$  and  $q_{ai}$  variables just as in the density evolution approach. We will call the combination of a Tanner graph and the  $p$  and  $q$  variables a “decorated Tanner graph.” The heart of the RG approach is the RG transformation, by which we eliminate (“renormalize away”) one node in the decorated Tanner graph, and adjust the remaining values of the  $p$  and  $q$  messages so that the new code

has a decoding failure rate as close as possible to the old code. With each renormalization step, the decorated Tanner graph representing our code will thus shrink by one node, until it is finally small enough that the performance of the code can be computed exactly in an efficient way.

We will explain all the details in the following sub-sections, but in general, the RG algorithm will work as follows:

1. Choose a “target” variable node  $i$  for which we want to compute the decoding failure rate  $b_i$ .
2. While the number of nodes remaining in the graph is greater than the number that one can comfortably handle exactly, repeatedly renormalize away nodes from the graph according to the following procedure:
  - (a) Mark the “distance” of every node from the “target” node. The distance between two nodes is the minimal number of nodes that one needs to pass through on the graph to travel from one node to the other.
  - (b) As long as there are any “leaf” (a *leaf* is a node which is only connected to one other node in the graph) check or variable nodes, renormalize them away. The order in which they are renormalized away will not matter, but for concreteness, we will renormalize those furthest from the “target” node first, breaking ties randomly.
  - (c) Otherwise, choose a single variable node from among those furthest from the target node, that has the fewest neighboring check nodes, and renormalize it away.
3. Compute  $b_i$  for the remaining graph exactly.

It should be clearly understood that the RG approach is approximate, and that there exists considerable freedom in the implementation. Different choices made in the implementation will lead to slightly different results. One can deal with this problem by constructing a series of systematically better RG approximations that should eventually converge to the exact answer. We shall see how this works out in our case in section 3.4. In the physics literature, this type of approach is well-known; the interested reader should consult the book [19].

### 3.2 The RG transformation for Tanner graphs with no loops

First we consider loop-free Tanner graphs, and write down the RG transformations that are sufficient to give exact results for such codes. In later subsections, we will extend the RG transformations in order to obtain good approximate results for Tanner graphs with loops.

We will always initialize our decorated Tanner graph such that all  $b_i = x$ ,  $p_{ia} = x$  and all  $q_{ai} = 0$ . Imagine that we are interested in the decoding failure rate  $b_i$  at a specific node  $i$ . Our procedure will be to obtain  $b_i$  by repeatedly renormalizing away nodes, other than the variable node  $i$  itself, that are “leaves” of the decorated Tanner graph.

The first possibility that we need to concern ourselves with is when we renormalize away a “leaf” variable node  $i$  that is connected to a single check node  $a$ . Clearly, when the node  $i$  vanishes,  $p_{ia}$  and  $q_{ai}$  will also be discarded. We need to renormalize all the  $q_{aj}$  variables leading out of the check  $a$  to other nodes  $j$ . Our formula will be

$$q_{aj} \leftarrow 1 - (1 - q_{aj})(1 - p_{ia}) \quad (38)$$

where the left arrow indicates that we replace the old value of  $q_{aj}$  with this new value. Notice that each renormalization of  $q_{aj}$  will increase its value.

When we renormalize away a “leaf” check node  $a$  that is only connected to a single variable node  $i$ , we need to adjust the values of all the  $p_{ib}$  variables leading to other checks  $b$  that node  $i$  is attached to. The renormalization group transformation will be

$$p_{ib} \leftarrow p_{ib}q_{ai}. \quad (39)$$

Notice that each renormalization of  $p_{ib}$  will decrease its value. At the same time, we should also renormalize the  $b_i$  as follows:

$$b_i \leftarrow b_iq_{ai}. \quad (40)$$

When only the “target” node  $i$  remains, we can just read off the current value of  $b_i$  and that will serve as the RG prediction.

### 3.3 A small example

The RG procedure might be easier to understand if we work through a small example. Recall the code defined by the parity check matrix

$$A = \begin{pmatrix} 1 & 1 & 0 & 0 \\ 0 & 1 & 1 & 1 \end{pmatrix}. \quad (41)$$

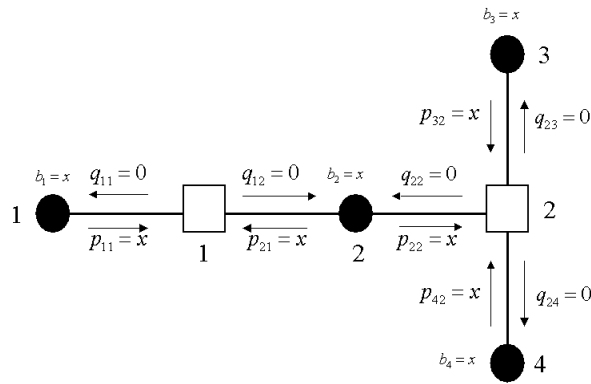


Figure 3: Decorated Tanner graph

Let us imagine that we would like to compute the decoding failure rate at the second variable node  $b_2$ . We initialize  $p_{11} = p_{21} = p_{22} = p_{32} = p_{42} = x$ ,  $q_{11} = q_{12} = q_{22} = q_{23} = q_{24} = 0$ , and  $b_2 = 0$ . In figure 3, we show the decorated Tanner graph for this code. All of the variable nodes other than variable node 2 are leaf nodes, so we can renormalize any of them away. According to our general algorithm, we should renormalize away the one furthest from node 2, breaking ties randomly. Let's say we choose variable node 4. Then we discard  $p_{42}$  and  $q_{24}$  and obtain new values  $q_{22} = x$  and  $q_{23} = x$  using equation (38). The new decorated Tanner graph is shown in figure 4. Let's next renormalize away variable node 3. We discard  $p_{32}$  and  $q_{23}$  and renormalize  $q_{22}$  to the value  $1 - (1 - x)^2 = 2x - x^2$ . The new decorated

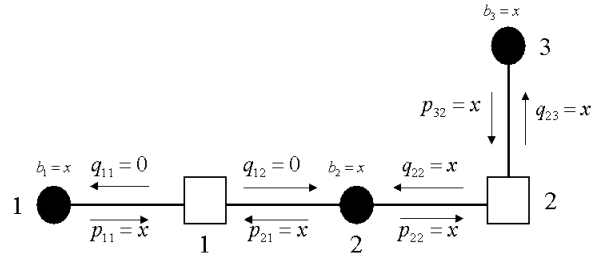


Figure 4: Decorated Tanner graph after renormalizing variable node 4.

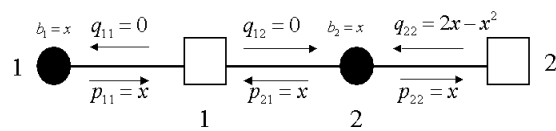


Figure 5: Decorated Tanner graph after renormalizing variable nodes 3 and 4.

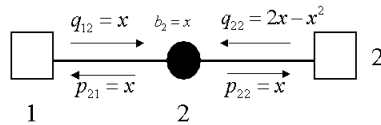


Figure 6: Decorated Tanner graph after renormalizing variable nodes 1, 3 and 4.

Tanner graph is shown in figure 5. Next we renormalize away variable node 1. We discard  $p_{11}$  and  $q_{11}$  and obtain the new renormalized value  $q_{12} = x$ ; the Tanner graph is now shown if figure 6. Next we renormalize away check node 2. We can discard  $p_{22}$  and  $q_{22}$  and obtain  $p_{21} = b_2 = 2x^2 - x^3$  (shown in figure 7.) Finally we renormalize away check node 1. We are left with only a single node (our original node 2) and  $b_2$  gets renormalized to its correct value  $b_2 = 2x^3 - x^4$ .

This example makes it clear why the RG approach is exact for a code defined on a graph without loops: the RG transformations essentially reconstruct the density evolution equations, and we know that density evolution is exact for such codes. As we shall see, the advantage of the RG approach is that it still gives a good approximation for codes defined on graphs with loops.

### 3.4 The RG approach for a graph with loops

For a code defined a graph that has loops, we will eventually have to renormalize away a variable node  $i$  that is not a “leaf” node. (Note that we could

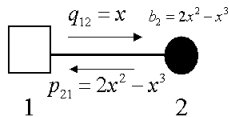


Figure 7: Decorated Tanner graph after renormalizing variable nodes 1, 3 and 4, and check node 2.

also renormalize away non-leaf check nodes by defining the appropriate RG transformations, but we will choose instead to always renormalize away non-leaf variable nodes.) To do that, we first collect all the check nodes  $a$ ,  $b$ , etc., that node  $i$  is attached to. Obviously, we will discard  $q_{ai}$ ,  $q_{bi}$ ,  $p_{ia}$ ,  $p_{ib}$ , etc. For any given check node attached to  $i$  (say check node  $a$ ), we must also collect all the other variable nodes  $j$  attached to  $a$ , and renormalize the values of  $q_{aj}$ . In figure 8, we illustrate the process of removing a non-leaf node.

The renormalization of the  $q_{aj}$  variable can be done to varying degrees of accuracy. The simplest approach would be to use equation (38) directly. The problem with this approach is that the value of  $p_{ia}$  which is used will always be an over-estimate. Recall that  $p_{ia}$  decreases with every renormalization. Since we are renormalizing away the  $i$ th node before it has become a leaf node,  $p_{ia}$  has not yet been fully renormalized, and is thus over-estimated.

Instead of using  $p_{ia}$  directly, we could use the value that it would have after we renormalized away all the checks connected to it; that is we could

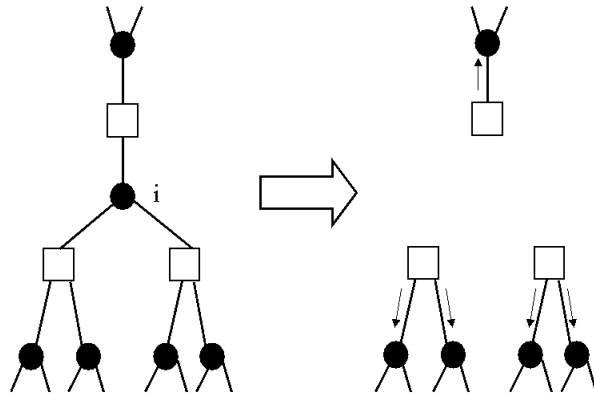


Figure 8: Removing the non-leaf node  $i$ . The arrows indicate the  $q$  variables that will be renormalized as a result.

replace  $p_{ia}$  in equation (38) with an effective  $p_{ia}^{\text{eff}}$  given by

$$p_{ia}^{\text{eff}} = p_{ia} \prod_{b \in N(i) \setminus a} q_{bi}. \quad (42)$$

On the other hand, we know that the values of the  $q_{bi}$  are *under-estimates* since they have not yet been fully renormalized either, so  $p_{ia}^{\text{eff}}$  as written above would also be an under-estimate. We could attempt to correct this mistake by going further another level: before we estimate a  $p_{ia}^{\text{eff}}$ , we first re-estimate the  $q_{bi}$  which feed into it. Thus, we replace the  $p_{ia}$  in equation (38) with an effective  $p_{ia}^{\text{eff}}$  given by

$$p_{ia}^{\text{eff}} = p_{ia} \prod_{b \in N(i) \setminus a} q_{bi}^{\text{eff}}, \quad (43)$$

where  $q_{bi}^{\text{eff}}$  is in turn given by

$$q_{bi}^{\text{eff}} = 1 - (1 - q_{bi}) \prod_{k \in N(b) \setminus i} (1 - p_{kb}). \quad (44)$$

Putting all these together, we finally get the RG transformation

$$q_{aj} \leftarrow 1 - (1 - q_{aj}) \left( 1 - p_{ia} \prod_{b \in N(i) \setminus a} \left[ 1 - (1 - q_{bi}) \prod_{k \in N(b) \setminus i} (1 - p_{kb}) \right] \right) \quad (45)$$

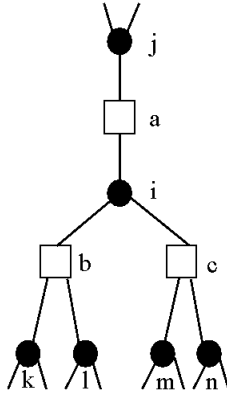


Figure 9: Node  $i$  sees a local tree-like structure.

The RG transformation (45) is worth explaining in more detail. In figure 9, we illustrate the equation for a case where variable node  $i$  is attached to three checks node  $a$ ,  $b$ , and  $c$ , and check node  $a$  is in turn attached to a variable node  $j$ . Check nodes  $b$  and  $c$  in turn are connected to their own variable nodes labeled  $k$ ,  $l$ ,  $m$ , and  $n$ . We would like to know the new probability  $q_{aj}$  that check node  $a$  will send variable node  $j$  an erasure message, taking into account the information that flows through node  $i$ . We already have some previous accumulated probability  $q_{aj}$  that check node  $a$  sends variable node  $j$  an erasure message (because of other nodes previously attached to  $a$  that have already been renormalized). The new probability of an erasure message can be figured out from a logical argument: “ $m_{aj}$  will be an erasure it was already, **or** if  $m_{ia}$  is an erasure **and** ( $m_{bi}$  **or**  $m_{kb}$  **or**  $m_{lb}$  are erasures) **and** ( $m_{ci}$  **or**  $m_{mc}$  **or**  $m_{nc}$  are erasures).” Converting such a logical argument into an equation for probabilities is straightforward: when we see “ $m_1$

**and**  $m_2$ ” for two statistically independent messages in a logical argument, it translates to  $(p_1 p_2)$  for the corresponding probabilities, while “ $m_1$  **or**  $m_2$ ” translates to  $(1 - (1 - p_1)(1 - p_2))$ . Converting our full logical argument for figure 4 into an equation for probabilities, we thus recover an example of the RG transformation (45).

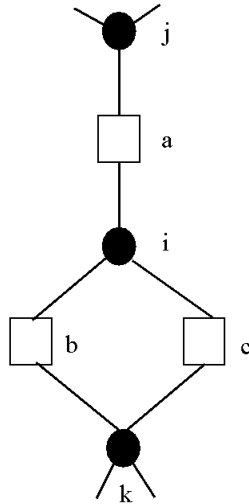


Figure 10: Node  $i$  sees a local neighborhood with loops.

We should always take our RG transformation for  $q_{aj}$  to correspond to the logic of the local neighborhood around the node  $i$  that we are removing. In fact, the RG transformation given in equation (45) is only appropriate if the local neighborhood of node  $i$  is tree-like, and must be corrected if there are short loops in the local neighborhood. For example, in figure 10, we illustrate a case where a variable node  $k$  is attached to two check nodes  $b$  and  $c$  which are each attached to the node  $i$  that we plan to remove. First consider the renormalization of  $q_{aj}$ . Note that before check nodes  $b$  or  $c$  are renormalized, the probabilities  $p_{kb}$  and  $p_{kc}$  that variable node  $k$  sends out an erasure must be identical, because all renormalizations of  $p_{kb}$  and  $p_{kc}$  happen in tandem. Our logic argument for whether check node  $a$  will send variable node  $j$  an erasure message would thus be: “ $m_{aj}$  will be an erasure if it was already, **or** if ( $m_{ia}$  is an erasure) **and** (( $m_{kb}$  is an erasure) **or** ( $m_{bi}$  **and**  $m_{ci}$  are erasures)).”

(We have used the fact that at this stage in the renormalization process, if  $m_{kb}$  is an erasure,  $m_{kc}$  must be as well.) Converting our logic argument into an RG transformation, we get

$$q_{aj} \leftarrow 1 - (1 - q_{aj})(1 - p_{ia}(1 - (1 - p_{kb})(1 - q_{bi}q_{ci}))) \quad (46)$$

The appropriate renormalizations of  $q_{bk}$  and  $q_{ck}$  are more complicated: the messages  $m_{bk}$  and  $m_{ck}$  are correlated because of node  $i$ , and we must keep track of that correlation after node  $i$  is removed. We have tried several relatively ad-hoc rules for assigning renormalized values to  $q$ 's that all arrive at the same node (such as renormalizing the product  $q_{bk}q_{ck}$  as a whole), but found the results to be unsatisfactory because they depended sensitively on the details of the rules. In general, to correctly account for the correlations caused by such short loops, we shall need to introduce additional variables beyond the  $q$  and  $p$  variables that we use here. We defer a detailed discussion of this complex issue to another paper [20]. In this paper, we will restrict our examples to codes where the local structure is always tree-like and such short loops do not exist.

The procedure we are describing for renormalizing a non-leaf variable node  $i$  can be made increasingly accurate by increasing the size of the neighborhood around the node  $i$  that is treated correctly. Naturally, as we increase the size of the neighborhood, we must pay for the increased accuracy with greater computation. We will use the following terminology: if, when renormalizing the node  $i$ , we use the values of  $p_{ia}$  directly, we will say that the resulting RG transformations have “depth” of one. If we first adjust the values of  $p_{ia}$  by considering all the check nodes  $a$  attached to  $i$  and all the variable nodes  $k$  attached to those check nodes, we will say the resulting RG transformations (e.g. those described above) have a depth of two. If we go one step further and also consider the check nodes attached to the variable nodes  $k$  and the variable nodes attached to those check nodes, we say the RG transformations have a depth of three, and so on.

### 3.5 Finishing the RG computation exactly

In the RG approach, we can always renormalize nodes away until we are left with just our “target” node  $i$ , and then read off the decoding failure rate for that node  $b_i$ . On the other hand, after we have renormalized away enough nodes, we could just as well finish the computation exactly.

For the purposes of describing the exact computation, we assume that we are given a Tanner graph of  $N$  nodes, and associated with each node  $i$  is an erasure probability  $x_i$ . (This is a little different from the decorated Tanner graph we are used to dealing with, but we shall show how to convert a Tanner graph into such a form.) To exactly compute the decoding failure rate of a given node  $i$ , we generate all  $2^N$  possible received message blocks (ranging from the correct all-zeros message all the way to the all-erasures message), and decode each of them using a BP decoder. Each message block has a probability

$$p = \prod x_i \prod (1 - x_j) \quad (47)$$

where the first product is over all nodes that are erased and the second product is over all nodes that are not erased. We simply compute  $b_i$  by taking the weighted average over all received messages of the probability that node  $i$  decodes to an erasure. Of course, the complexity of the exact calculation is  $O(2^N)$ , so we are restricted to small  $N$ , but nevertheless one can gain some accuracy by switching to an exact calculation after one has renormalized away enough nodes.

The one subtlety in the exact final calculation is that one needs a Tanner graph and the associated erasure probabilities at each node, but in the RG approach, we manipulate decorated Tanner graphs. Fortunately, it is easy to convert a decorated Tanner graph into the appropriate form. Note that at each step of the RG approach, all the probabilities  $q_{ai}$  leading out of the check node  $a$  must be equal (we say  $q_{ai} = q_a$ ) and all the probabilities  $p_{ia}$  leading out of the variable node  $i$  will be equal (we say  $p_{ia} = p_i$ ). We can set all the  $q_a$  probabilities equal to zero if we expand the graph by adding a new variable node  $k$  to node  $a$  with  $p_{ka} = q_a$ . When we are left with a decorated Tanner graph such that all  $q$  probabilities are zero, and all  $p_{ia}$  probabilities coming out of each variable node are equal to  $p_i$ , we may interpret the  $p_i$  as the erasure probabilities of the variable nodes. In figure 11, we give an example of expanding a decorated Tanner graph into an equivalent Tanner graph with erasure probabilities.

### 3.6 Extension to generalized parity check matrices

Many of the best modern codes, such as turbo-codes, Kanter-Saad codes, and repeat-accumulate codes, are easily represented in terms of *generalized* parity

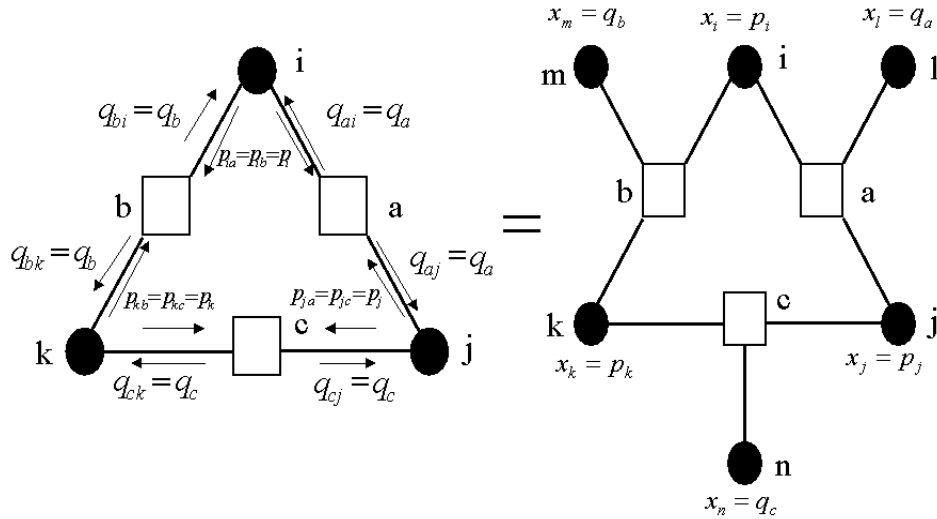


Figure 11: Expanding a decorated Tanner graph into an equivalent Tanner graph with erasure probabilities.

check matrices [2]. In a generalized parity check matrix, additional columns are added to a parity check matrix which represent “hidden nodes”—state variables which are not transmitted. A good notation for the state variables is a horizontal line above the corresponding columns. For example, we would write

$$A = \begin{pmatrix} \bar{1} & 1 & 0 & 1 & 0 & 0 \\ 1 & 0 & 1 & 0 & 1 & 0 \\ 0 & 1 & 1 & 0 & 0 & 1 \end{pmatrix} \quad (48)$$

to indicate a code where the first variable node was a hidden node. To indicate that a variable node is a hidden node in our graphical model, we use an open circle rather than a filled-in circle. Such a graph, which generalizes Tanner graphs, is called a “Wiberg graph” [21, 22]. In figure 12, we give the

Wiberg graph corresponding to the code defined by the generalized parity check matrix (48).

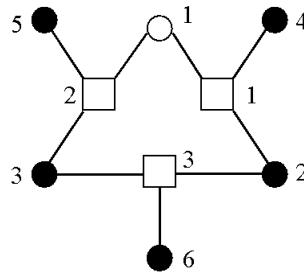


Figure 12: A Wiberg graph.

The generalization of our RG procedure to handle Wiberg graphs is very straightforward. We initialize the probabilities  $p_{ia}$  coming out of a hidden node at 1, instead of at the erasure rate  $x$  as we do for ordinary transmitted variable nodes. This reflects the fact that hidden nodes are automatically erased, while ordinary variable nodes are only erased with probability  $x$ .

## 4 Comparison with numerical simulations

We now present a comparison of the predictions of our RG approach with numerical simulations. We first used a parity check matrix corresponding to a  $(3, 5)$  regular Gallager code with  $N = 60$  and  $k = 24$ . That is, each of the 36 rows in the parity check matrix had 5 entries that were ones (the rest were zeros), and each of the 60 columns had 3 entries which were zeros. There were no hidden nodes.

We also took care to ensure that no two parity checks shared more than one variable node. That meant that there were no loops of length four, so we

could use the RG transformation (45) (an RG transformation of “depth” 2) whenever we renormalized away a non-leaf variable node. We renormalized nodes away until we were left with 7 nodes, and then finished the computation exactly.

We considered erasure rates  $x$  at intervals of .05 between  $x = 0$  and  $x = 1$ . When we used the RG approximation, we averaged our decoding failure rates  $b_i$  over all 100 nodes  $i$  to get an overall bit error rate. Our numerical simulations consisted of 1000 trials at each erasure rate, decoded according to the standard BP decoding algorithm.

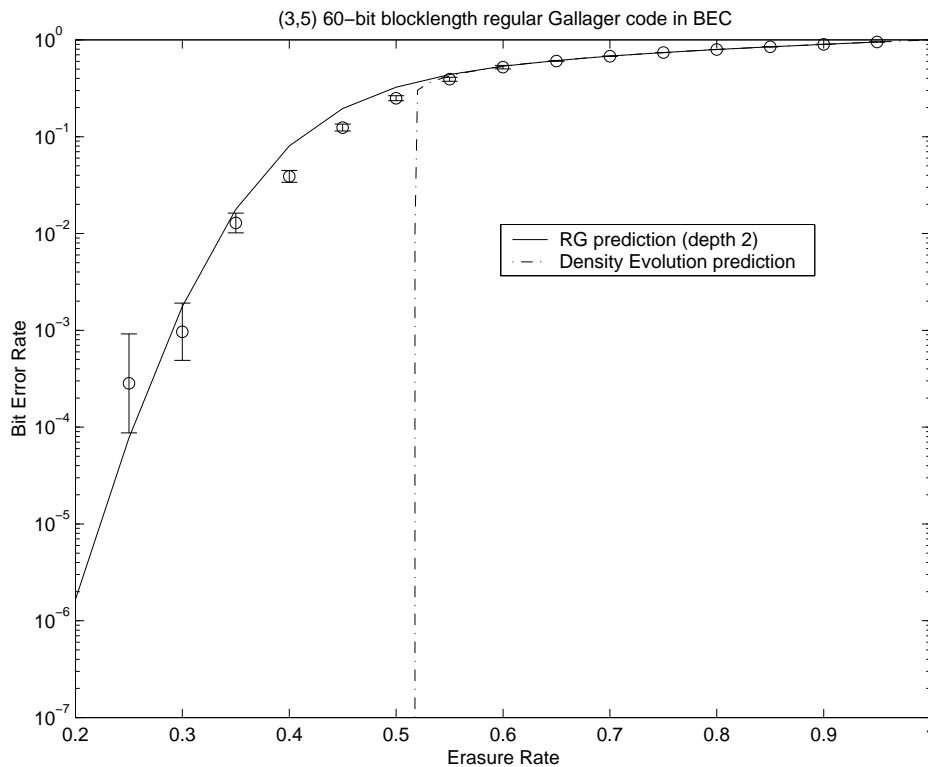


Figure 13: Simulation results compared with RG and density evolution predictions for a small rate  $2/5$  60-bit blocklength regular Gallager code.

Our results are presented in figure 13, where we compare the simulation results with the prediction of our RG approach and the density evolution approach. As one can see, the agreement between the RG approach and

simulations is quite good.

The density evolution prediction is precisely the same as it would be in the infinite-blocklength limit. Of course, nobody claims that the density evolution approach should be taken seriously for blocklengths as low as 60, and figure 13 shows why: the density-evolution prediction of a threshold-like behaviour is completely incorrect for small or medium blocklength regular Gallager codes.

We then constructed, by a somewhat random procedure, a particular irregular Gallager code of rate  $2/5$  and blocklength  $N = 100$ . Each variable node belonged to between one and four parity checks, and each parity check involved between three and five variable nodes. No special effort was made to construct a particularly good error-correcting code, but we did ensure that the Tanner graph had no short loops of length four or six (counting both variable and check nodes). That meant that all local neighborhoods could be considered tree-like up to RG transformations of depth 3.

Our procedures were the same as described for the regular Gallager code except that we implemented RG transformations of depth 1, 2, and 3. Our numerical simulations consisted of 5000 trials for all erasure rates  $x \leq .6$ , and 1000 trials for higher erasure rates.

In figure 14, we compare the simulation results with the prediction of our RG approach for the bit error rate averaged over all nodes. As one can see, the agreement is remarkably good, especially for the RG transformations of depth 3. The density evolution prediction spuriously shows a quasi-threshold behavior around  $x \approx .555$ .

The irregular Gallager code has interesting variation in its bit error rates across the different bits of the code. In figure 15 we plot the predicted (using depth 3 RG transformations) and simulated bit error rates for every bit in the code at an erasure rate of  $x = .55$ . This plot demonstrates that the RG approach can in fact predict the bit-by-bit variation in the bit error rate. Although the RG prediction is systematically slightly too high at this erasure rate, it captures the ordering of how easily the bits are decoded quite well.

## 5 Extension to the Gaussian noise channel.

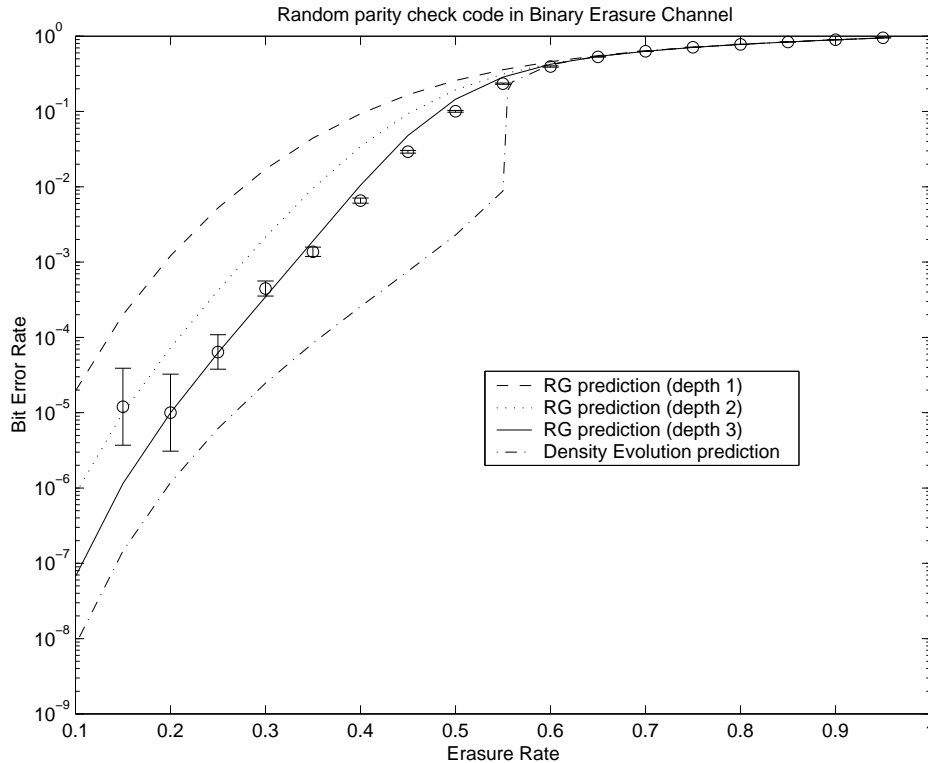


Figure 14: Simulation results compared with RG predictions using depths from one to three and density evolution predictions for a small rate  $2/5$  100-bit blocklength irregular Gallager code.

## 5.1 Background

In this section, we consider the extension of the RG approach to the additive white Gaussian noise (AWGN) channel. We will build on the Gaussian approximation to density evolution for the AWGN channel described by Chung, et. al. [23], so we first describe that approximation.

In the AWGN channel, there are only two possible inputs, 0 and 1, but the output alphabet is the set of real numbers: if  $x$  is the input, then the output would be  $y = (-1)^x + z$ , where  $z$  is a Gaussian random variable with zero mean and variance  $\sigma^2$ . For each received bit  $i$  in the code, we can compute the log-likelihood ratio  $m_i^0 = \ln(p(y_i|x_i = 0)/p(y_i|x_i = 1))$  which tells us the relative log-likelihood ratio that the transmitted bit  $i$  was a zero

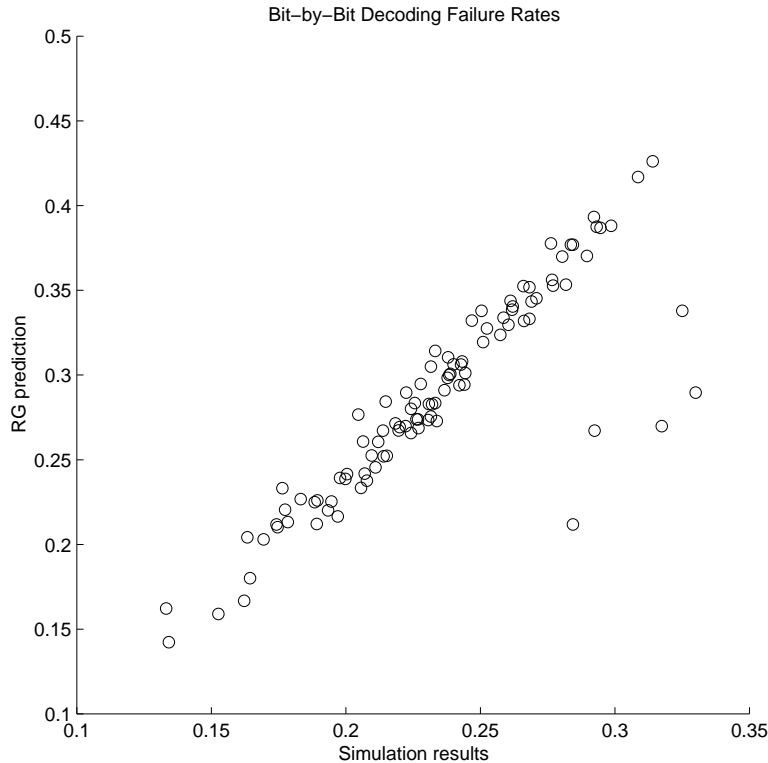


Figure 15: Bit-by-bit comparison of simulation results and RG predictions for a small rate  $2/5$  100-bit blocklength irregular Gallager code at an erasure rate of  $x = .55$  in the BEC.

given the received real number is  $y_i$ .

We assume that we are again dealing with codes defined by generalized parity check matrices, that we always transmit the all-zeros codeword, and that the decoding algorithm is the sum-product belief propagation algorithm. In this decoding algorithm, we iteratively solve for real-valued messages:  $m_{ia}$  from variable nodes  $i$  to check nodes  $a$ ; and  $m_{ai}$  from check nodes  $a$  to variable nodes  $i$ . The messages  $m_{ia}$  are log-likelihood ratios by which the node  $i$  informs the node  $a$  of its probability of being a 0 or 1. For example,  $m_{ia} \rightarrow \infty$  means that node  $i$  is certain it should be a 0, while  $m_{ia} = 1$  means that variable node  $i$  is telling check node  $a$  that  $\ln(p(x_i = 0)/p(x_i = 1)) = 1$ . The messages  $m_{ai}$  are log-likelihood ratios which should be interpreted as

information from the check node  $a$  to the variable node  $i$  about what state node  $i$  should be in.

In the sum-product algorithm, the messages are iteratively solved according to the update rules:

$$m_{ia} = \sum_{b \in N(i) \setminus a} m_{bi} + m_i^0 \quad (49)$$

(if  $i$  is a hidden node, the  $m_i^0$  term is omitted) and

$$\tanh(m_{ai}/2) = \prod_{j \in N(a) \setminus i} \tanh(m_{ja}/2). \quad (50)$$

In the density evolution approach for the AWGN channel, one considers the probability distributions  $p(m_{ia})$  and  $p(m_{ai})$  for the messages where the probability distribution is an average over all possible received blocks. A distribution  $f(x)$  is called *consistent* if  $f(x) = f(-x)e^x$  for all  $x$  [9]. Richardson and Urbanke [16] proved that the consistency condition will be preserved for the message probability distributions for all messages under sum-product decoding. If we approximate the probability distributions  $p(m_{ia})$  and  $p(m_{ai})$  as Gaussian distributions, the consistency condition means the means  $\mu$  of these distributions will be related to the variances  $\sigma^2$  by  $\sigma^2 = 2\mu$ . That means that we can characterize the message probability distributions by a single parameter: their mean.

Thus, by making the approximation that the message probability distributions are Gaussians, one can reduce the density evolution equations for the AWGN channel to self-consistent equations for the means  $u_{ia}$  of the probability distributions of messages from variable nodes  $i$  to check nodes  $a$ , and the means  $v_{ai}$  of the probability distributions of messages from check nodes  $a$  to variable nodes  $i$ . These equations are

$$v_{ia} = u_i^0 + \sum_{b \in N(i) \setminus a} u_{bi} \quad (51)$$

where  $u^0$  is the mean value of  $m_i^0$  (this term is omitted for hidden nodes), and

$$\phi(u_{ai}) = 1 - \prod_{j \in N(a) \setminus i} (1 - \phi(v_{ja})) \quad (52)$$

where  $\phi(x)$  is a function defined by

$$\phi(x) \equiv 1 - \frac{1}{\sqrt{4\pi x}} \int_{-\infty}^{\infty} \tanh \frac{u}{2} e^{-\frac{(u-x)^2}{4x}} du \quad (53)$$

$\phi(x)$  can be approximated in a form that reproduces the correct limits as  $x \rightarrow 0$  and  $x \rightarrow \infty$  and is more convenient for numerical purposes. We choose

$$\phi(x) \approx \frac{e^{-x/4}}{\sqrt{1+\beta x}} \left[ 1 + (\sqrt{\beta\pi - 1}) \frac{\alpha x}{1 + \alpha x} \right] \quad (54)$$

This form automatically has the correct leading behavior as  $x \rightarrow 0$  and  $x \rightarrow \infty$  for any  $\alpha$  and  $\beta$ . We fix  $\alpha$  and  $\beta$  by matching the leading corrections in the two limits. We find  $\alpha \approx 0.163489$  and  $\beta \approx 0.634765$ . This approximation to  $\phi(x)$  is quite good for all values of  $x$ .

## 5.2 RG transformations for the AWGN channel

The density evolution equations (51) and (52) for the AWGN channel under the Gaussian approximation are analogs of the density evolution equations (4) and (3) for the BEC channel. Our RG procedure for the AWGN channel will be almost exactly the same as for the BEC channel; the main difference is that we need to change the RG transformations.

Just as before, we can construct a set of RG transformations which exactly reproduce the density evolution equations for a tree-like graph. We create a decorated Tanner/Wiberg graph for the code by keeping  $u_{ai}$  and  $v_{ia}$  variables between each pair of connected nodes. The  $u_{ai}$  variables are initialized to  $\infty$ , while the  $v_{ia}$  variables are initialized to  $u^0$ , unless the  $i$ th node is a hidden node, in which case the  $v_{ia}$  are initialized to zero. We also introduce the variables  $h_i$  (analogous to  $b_i$  in the BEC) which are initialized like the  $v_{ia}$  variables.

If we renormalize away a leaf check node  $a$  attached to a check node  $i$ , we find the other check nodes  $b$  attached to  $i$  and apply the RG transformations

$$v_{ib} \leftarrow v_{ib} + u_{ai} \quad (55)$$

and

$$h_i \leftarrow h_i + u_{ai} \quad (56)$$

while if we renormalize away a leaf variable node  $i$  attached to a check node  $a$ , we find the other variable nodes  $j$  attached to  $a$  and apply the RG transformation

$$u_{aj} \leftarrow \phi^{-1} \left( 1 - (1 - \phi(u_{aj}))(1 - \phi(v_{ia})) \right) \quad (57)$$

Note that with each renormalization of  $v_{ib}$ , the magnitude of  $v_{ib}$  will increase, while with each renormalization of  $u_{aj}$ , the magnitude of  $u_{aj}$  will decrease.

When we renormalize away a non-leaf variable node  $i$  which is attached to check nodes  $a, b$ , etc., we need to renormalize the variables like  $u_{aj}$ , where  $j$  is another variable node attached to check node  $a$ . Just as for the BEC, we should consider a local neighborhood of nodes around the node  $i$ . For example, if no variable nodes  $j$  share two check nodes with  $i$  (there are no local loops of length four) then we can use the depth two RG transformation

$$u_{aj} \leftarrow \phi^{-1} \left( 1 - (1 - \phi(u_{aj}))(1 - \phi(v_{ia}^{\text{eff}})) \right) \quad (58)$$

where

$$v_{ia}^{\text{eff}} = v_{ia} + \sum_{b \in N(i) \setminus a} \phi^{-1} \left( 1 - (1 - \phi(u_{bi})) \prod_{k \in N(b) \setminus i} (1 - \phi(v_{kb})) \right) \quad (59)$$

The RG procedure proceeds as in the BEC case until the final computation of the bit error rate. For the AWGN channel, it will not normally be convenient to stop the RG procedure before renormalizing all the way down to the “target” node, because it is not simple to do an exact computation even with just a few nodes in the code. When we have renormalized all but our target node  $i$ , we will be left with a final renormalized value of  $h_i$ . Our Gaussian approximation tells us that the probability distribution for the node  $i$  being decoded as a zero will be a Gaussian with mean  $h_i$  and variance  $2h_i$ . Decoding failures correspond to those parts of the probability distribution which are below zero. Thus, our theoretical prediction for the bit error rate at node  $i$  will be

$$b_i = \frac{1}{\sqrt{8\pi h_i}} \int_{-\infty}^0 e^{-\frac{(x-h_i)^2}{4h_i}} dx. \quad (60)$$

## 6 Speculations on the design of codes

Given that the density evolution method has been used as a guide to designing the best-known practical codes, it is natural to expect that we could

design even better codes using the RG approach. With the RG approach, we can input a code defined by an arbitrary generalized parity check matrix, and obtain as output a prediction of the bit error rate at each node. We could use this output as the objective function for a guided search through the space of possible codes. For example, say that we would like to find a  $N = 100$  rate  $1/2$  code with no hidden states that achieves a bit error rate of less than  $10^{-4}$  at the smallest possible signal-to-noise ratio for the AWGN channel. We could repeatedly evaluate codes using the RG approach, and use any available search technique (greedy descent, simulated annealing, genetic algorithms, etc.) to search through the space of valid parity check matrices. Because we can directly focus on the correct figure of merit (the bit error rate itself, rather than the threshold in the infinite blocklength limit), one expects the search to improve on the results obtained using density evolution.

A couple of comments are in order. First, because we have information about the bit error rate at every node (see figure 15), we might be able to use that information to guide the search. For example, it might make sense to “strengthen” a variable node with a high bit error rate by adding it to more parity checks, or one could choose to “weaken” nodes with a low bit error rate by turning them into hidden nodes (thus increasing the rate).

On the other hand, computing the bit error rate of every node will obviously slow down a search. It may be worthwhile, at least for large blocklengths, to restrict oneself to those codes for which there are only a small number of different classes of nodes (defined in terms of the local neighborhoods of the nodes). Most of the best-known codes are of this type. Rather than computing the bit error rate for every variable node, one could then compute the bit error rate for just one representative of each class of variable node. For example, for a regular Gallager code, each node has the same local neighborhood, so any node can be chosen as a representative of all the nodes. The error made in this approach can be estimated by comparing bit error rates of different nodes of the same class. For actual finite-sized regular Gallager codes, we find that the RG approach will give very similar predictions for each of the nodes, so that the error made by just considering a single variable node as a representative of all of them is quite small.

## Acknowledgements

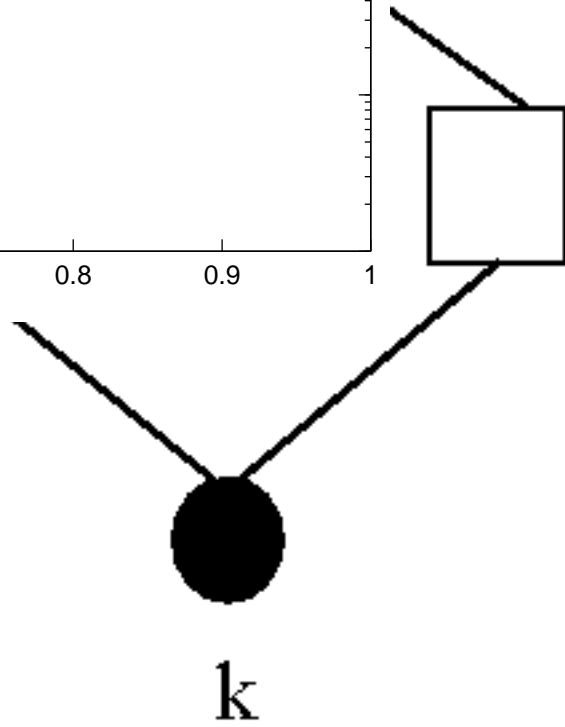
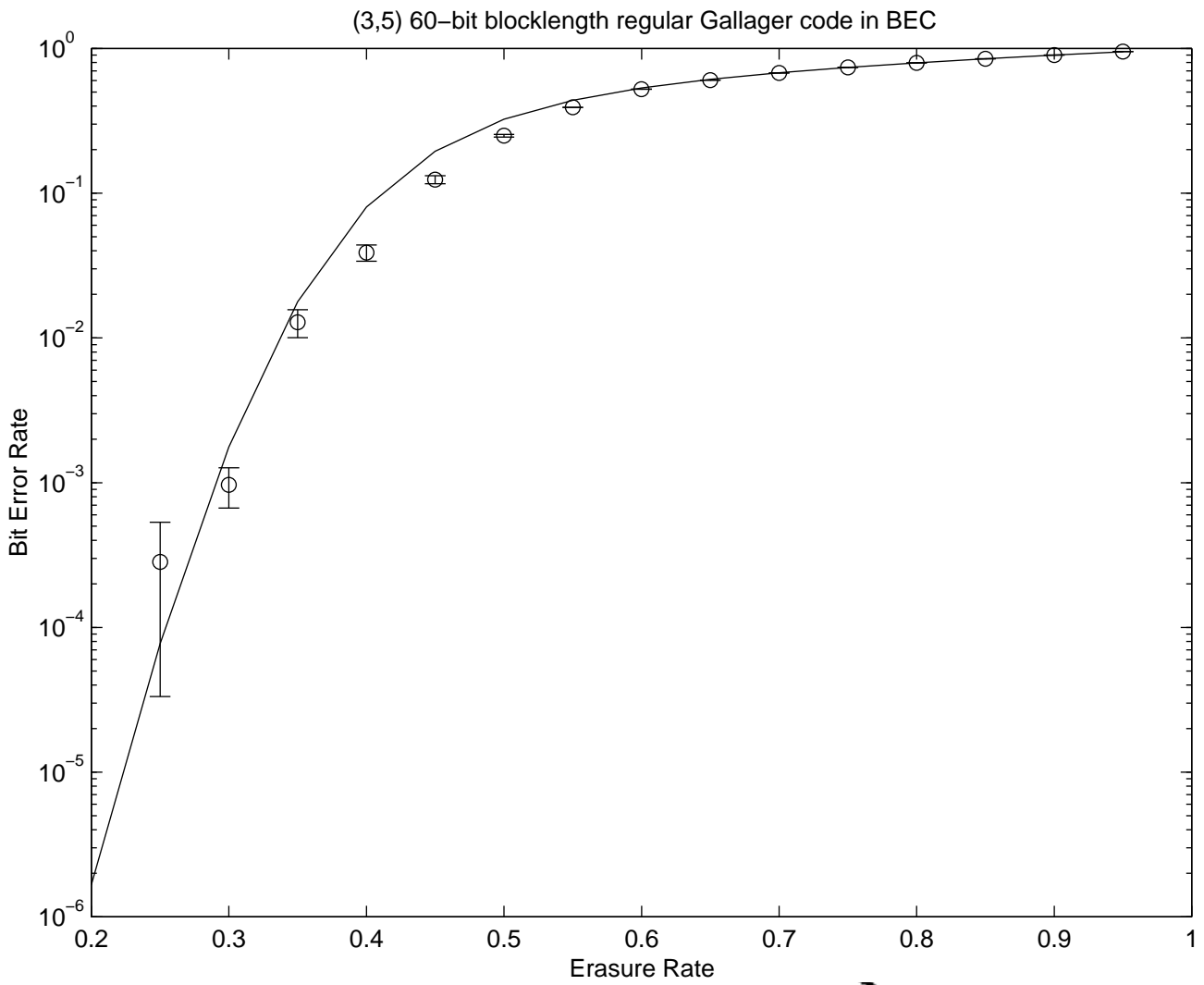
We thank Bill Freeman, Yair Weiss, Michael Mitzenmacher, Dave Forney, and David MacKay for helpful discussions. Jean-Philippe Bouchaud thanks Harvard University and Daniel Fisher for their hospitality during the period when this work was done.

## References

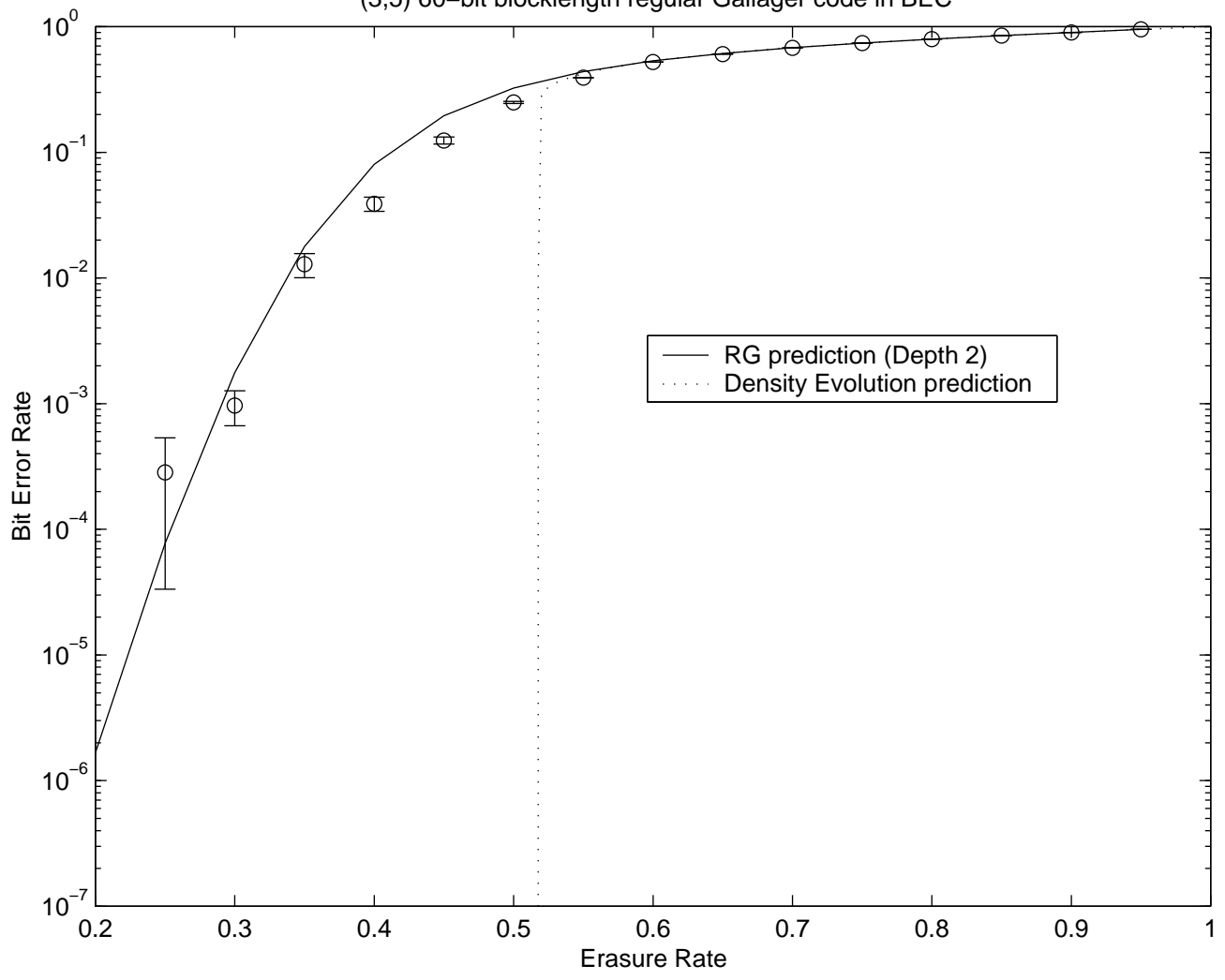
- [1] F. J. MacWilliams and N. J. A. Sloane. *The theory of error-correcting codes*. North-Holland, 1977.
- [2] D. J. C. Mackay. Relationships between sparse graph codes. In *(unpublished) proceedings of IBIS 2000, Japan*, 2000.
- [3] R. G. Gallager. *Low-density parity check codes*. MIT Press, 1963.
- [4] C. Berrou, A. Glavieux, and P. Thitimajshima. Near Shannon limit error-correcting coding and decoding: Turbo-codes. In *Proceedings 1993 IEEE International Conference on Communications*, pages 1064–1070, Geneva, Switzerland, 1993.
- [5] D. J. C. Mackay. Good error-correcting codes based on very sparse matrices. *IEEE Trans. Info. Theory*, 45:399–431, 1999.
- [6] M. G. Luby, M. Mitzenmacher, M. Amin Shokrollahi, D. A. Spielman, and V. Stemann. Practical loss-resilient codes. In *Proceedings of the Twenty-Ninth annual ACM Symposium on Theory of Computing (STOC)*, 1997.
- [7] M. G. Luby, M. Mitzenmacher, M.A. Shokrollahi, and D. A. Spielman. Improved low-density parity-check codes using irregular graphs. *IEEE Trans. Info. Theory*, 47(2):585–598, 2001.
- [8] Matthew C. Davey. *Error-correction using Low-Density Parity-Check Codes*. PhD thesis, Cambridge University, 1999.
- [9] T. J. Richardson, A. Shokrollahi, and R. L. Urbanke. Design of capacity-approaching irregular low-density parity-check codes. *IEEE Trans. Info. Theory*, 47(2):619–637, 2001.

- [10] S.-Y. Chung, G. D. Forney, T. J. Richardson, and R. L. Urbanke. On the design of low-density parity-check codes within 0.0045 db of the shannon limit. *IEEE Communications Letters*, 5:58–60, 2001.
- [11] I. Kanter and D. Saad. Error-correcting codes that nearly saturate shannon’s bound. *Physical Review Letters*, 83(13):2660–2663, 1999.
- [12] I. Kanter and D. Saad. Finite-size effects and error-free communication in gaussian channels. *Journal of Physics A*, 33:1675–1681, 2000.
- [13] D. Divsalar, H. Jin, and R. J. McEliece. Coding theorems for ‘turbo-like’ codes. In *Proceedings of the 36th Allerton Conference on Communication, Control and Computing*, pages 201–210, Allerton, Illinois, 1998.
- [14] H. Jin, A. Khandekar, and R. J. McEliece. Irregular repeat-accumulate codes. In *Proceedings 2nd International Symposium on Turbo codes and Related Topics*, pages 1–8, Brest, France, 2000.
- [15] R. J. McEliece, D. J. C. MacKay, and J. F. Cheng. Turbo decoding as an instance of Pearl’s ‘belief propagation’ algorithm. *IEEE J. on Sel. Areas in Comm.*, 16(2):140–152, 1998.
- [16] T. J. Richardson and R. L. Urbanke. The capacity of low-density parity-check codes under message-passing decoding. *IEEE Trans. Info. Theory*, 47(2):599–618, 2001.
- [17] L. Bazzi, T. J. Richardson, and R. L. Urbanke. Exact thresholds and optimal codes for the binary symmetric channel and Gallager’s decoding algorithm a. *IEEE Trans. Info. Theory*, 1999.
- [18] R. M. Tanner. A recursive approach to low complexity codes. *IEEE Trans. Info. Theory*, IT-27:533–547, 1981.
- [19] T. W. Burkhardt and J. M. J. Van Leeuwen. *Real Space Renormalization*. Springer-Verlag, 1982.
- [20] J. S. Yedidia and J.-P. Bouchaud. In preparation, 2001.
- [21] N. Wiberg. *Codes and decoding on general graphs*. PhD thesis, University of Linköping, 1996.

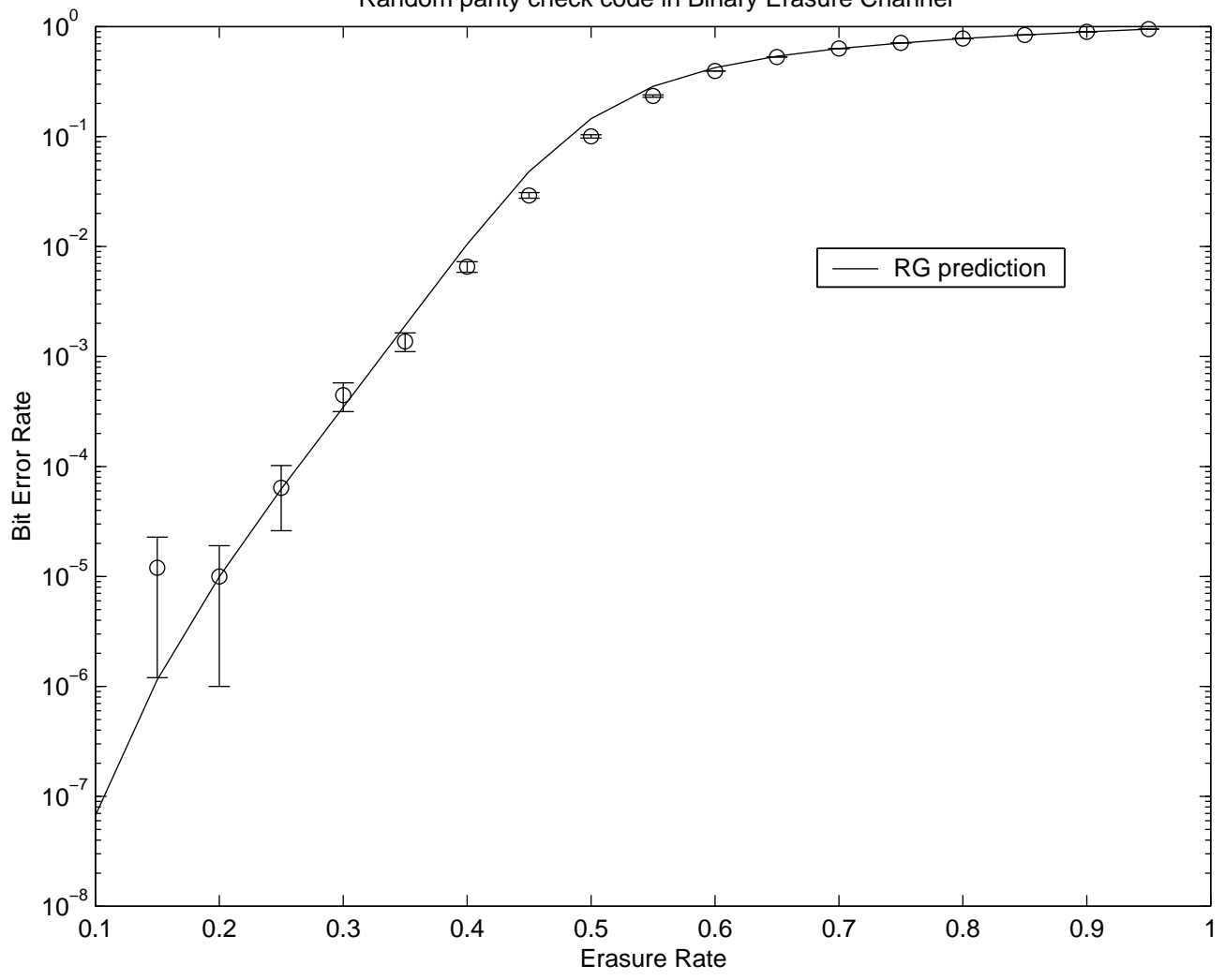
- [22] N. Wiberg, H.-A. Loeliger, and R. Kotter. Codes and iterative decoding on general graphs. *Euro. Trans. Telecomm.*, 6:513–525, 1995.
- [23] S.-Y. Chung, T. J. Richardson, and R. L. Urbanke. Analysis of sum-product decoding of low-density parity-check codes using a gaussian approximation. *IEEE Trans. Info. Theory*, 47(2):657–670, 2001.



(3,5) 60-bit blocklength regular Gallager code in BEC



Random parity check code in Binary Erasure Channel



Random parity check code in Binary Erasure Channel

